

CHAPTER 8

**RESULTS AND DISCUSSION: PHOSPHATE REMOVAL BY
OPC/FA AND OPC/SLAG**

8.1. Composition of the cement blends

The OPC/fly ash and OPC/slag samples used for the study were not blended in-house, but commercial products manufactured by Pretoria Portland Cement. The percentage of CaO in each of the blends as well as the pure constituents were determined by EDTA complexometric titrimetry after 1:4 fluxing with anhydrous $\text{Li}_2\text{B}_4\text{O}_7$, as described in Experimental Section 4.3.2. The data obtained are shown in Table 8.1.

Table 8.1. Composition of the OPC/FA and OPC/slag blends.

Adsorbent	% CaO	Calculated composition of blend
FA	4.5	
Slag	34.1	
OPC	63.8	
OPC/FA	57.3	OPC + 11 % FA
OPC/Slag	58.2	OPC + 19 % Slag

The experimentally obtained % CaO values were then used to calculate the composition of the blends using the expression (derived from first principles):

$$X \times \% \text{ CaO in FA (or slag)} + (100 - X) \times \% \text{ CaO in OPC} \\ = 100 \times \% \text{ CaO in OPC/FA (or OPC/slag) blend}$$

where X is the % FA (or slag) in the blend. The data are given in Table 8.1.

8.2. Kinetics

Figures 8.1 and 8.2 illustrate the percentage PO_4^{3-} removed with time by OPC/FA and OPC/slag respectively, measured as described in Experimental Section 4.3.4.

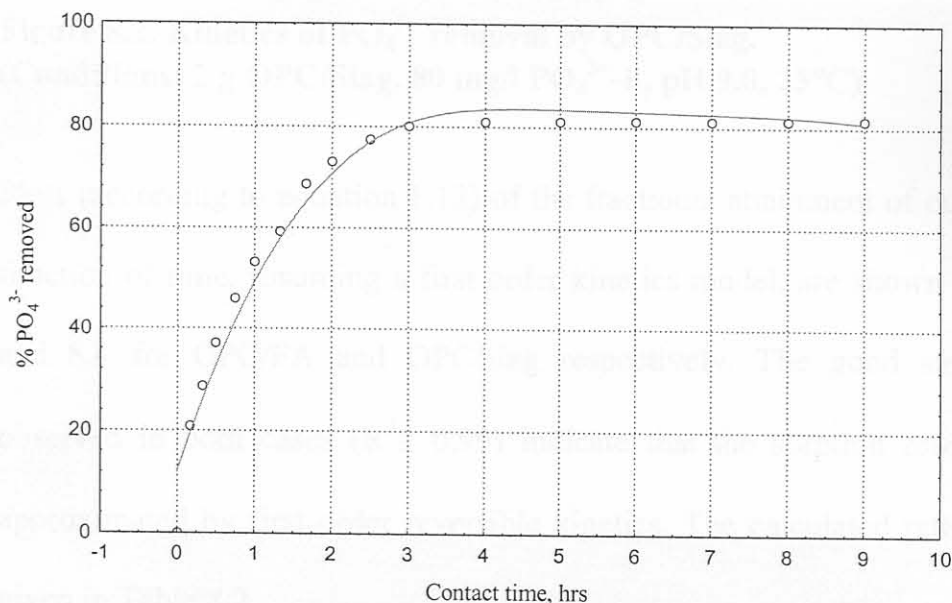


Figure 8.1. Kinetics of PO_4^{3-} removal by OPC/FA.
(Conditions: 2 g OPC/Fly ash, 80 mg/l PO_4^{3-} -P, pH 9.0, 25°C)

It can be seen that for both blends the uptake of PO_4^{3-} practically ceased after a contact time of about 3½ hrs, indicating the onset of dynamic equilibrium.

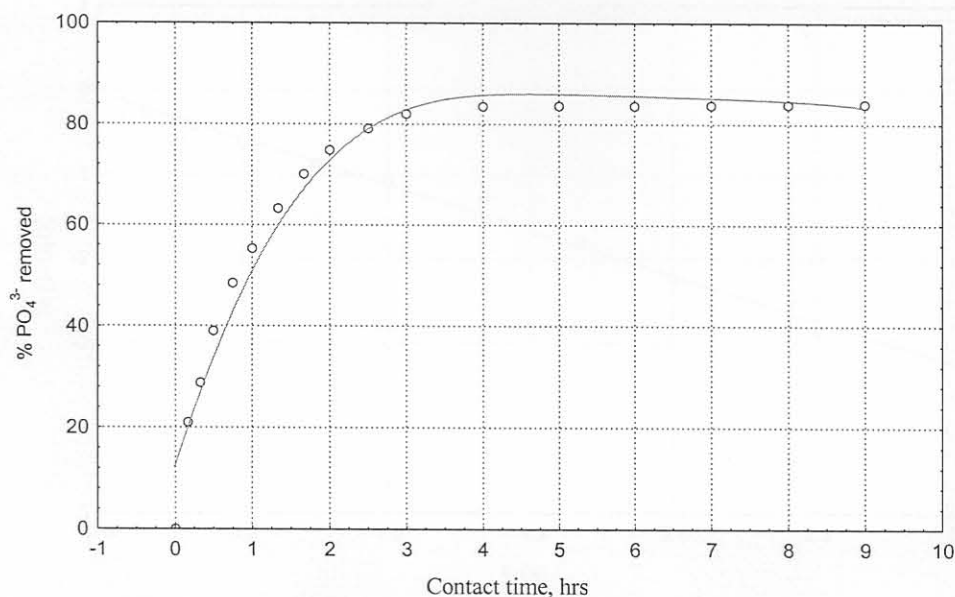


Figure 8.2. Kinetics of PO_4^{3-} removal by OPC/Slag.
(Conditions: 2 g OPC/Slag, 80 mg/l PO_4^{3-} -P, pH 9.0, 25°C)

Plots (according to equation 1.12) of the fractional attainment of equilibrium as a function of time, assuming a first order kinetics model, are shown in Figures 8.3 and 8.4 for OPC/FA and OPC/slag respectively. The good straight-line fits observed in both cases ($R^2 \cong 0.99$) indicate that the sorption reactions may be approximated by first order reversible kinetics. The calculated rate constants are given in Table 8.2.

Table 8.2. Values of first order reaction rate constants for PO_4^{3-} removal by OPC/FA and OPC/slag.

Adsorbent	k' (per hour)
OPC + 11 % FA	1.082
OPC + 19 % Slag	1.136

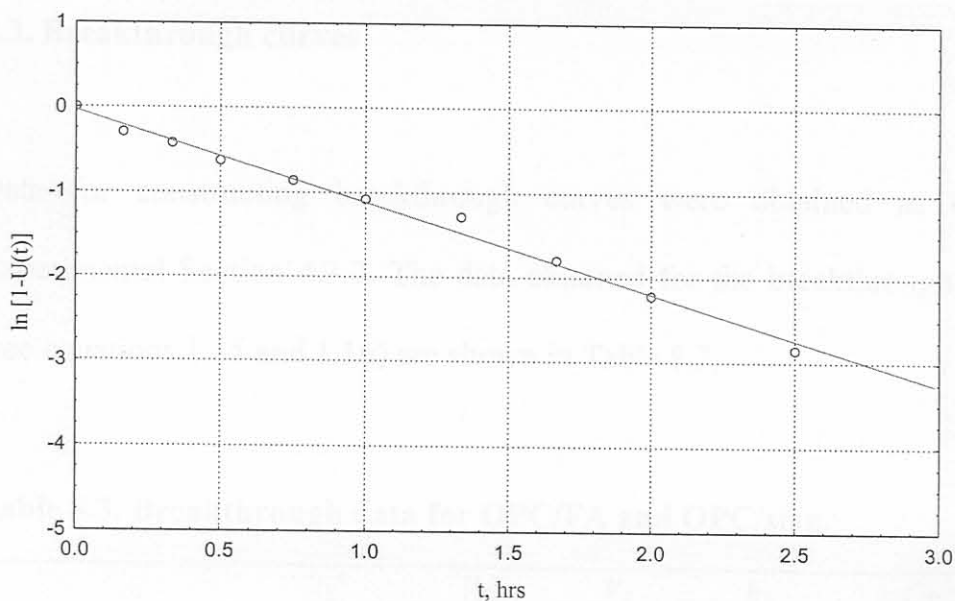


Figure 8.3. Application of first order kinetics to the experimental adsorption data for OPC/FA. (Conditions: 2 g OPC/FA, 80 mg/l $\text{PO}_4^{3-}\text{-P}$, pH 9.0, 25°C)

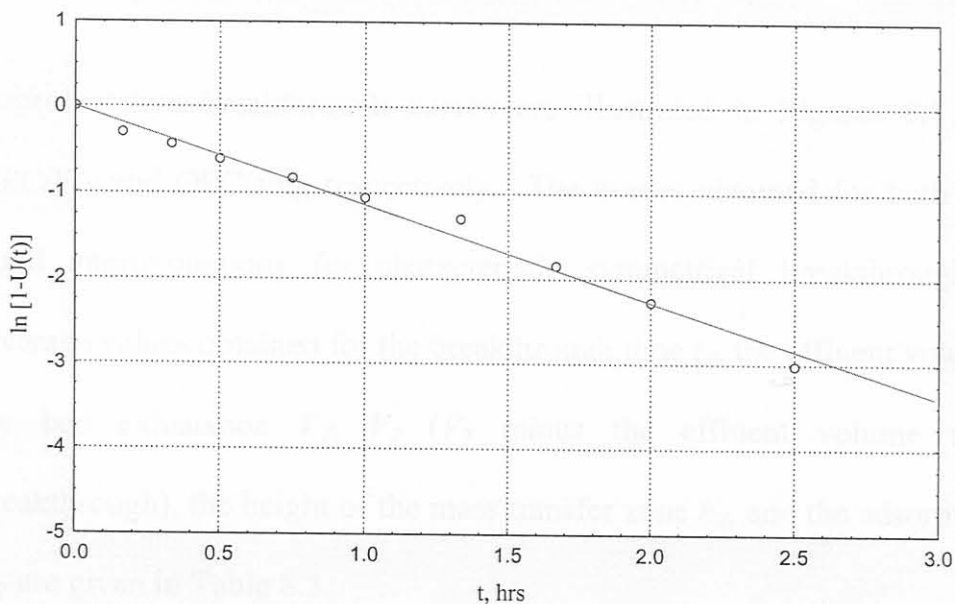


Figure 8.4. Application of first order kinetics to the experimental adsorption data for OPC/Slag. (Conditions: 2 g OPC/Fly ash, 80 mg/l $\text{PO}_4^{3-}\text{-P}$, pH 9.0, 25°C)

8.3. Breakthrough curves

Data for constructing breakthrough curves were obtained as described in Experimental Section 4.3.7. The data obtained for the breakthrough experiments (see equations 1.15 and 1.16) are shown in Table 8.3.

Table 8.3. Breakthrough data for OPC/FA and OPC/slag.

Adsorbent	t_E^a (min)	V_T (cm ³)	V_Z (cm ³)	h_Z (cm)	C_T (mg PO ₄ ³⁻ -P/g)
OPC + 11 % FA	9.4	375	139	0.910	75
OPC + 19 % Slag	9.9	388	140	0.881	78

^aBreakthrough time

Representative breakthrough curves are illustrated in Figures 8.5 and 8.6 for OPC/FA and OPC/slag respectively. The curves obtained for both blends were good approximations for characteristic symmetrical breakthrough S curves. Average values obtained for the breakthrough time t_E , the effluent volume required for bed exhaustion V_T , V_Z (V_T minus the effluent volume required for breakthrough), the height of the mass transfer zone h_Z , and the adsorption capacity C_T are given in Table 8.3.

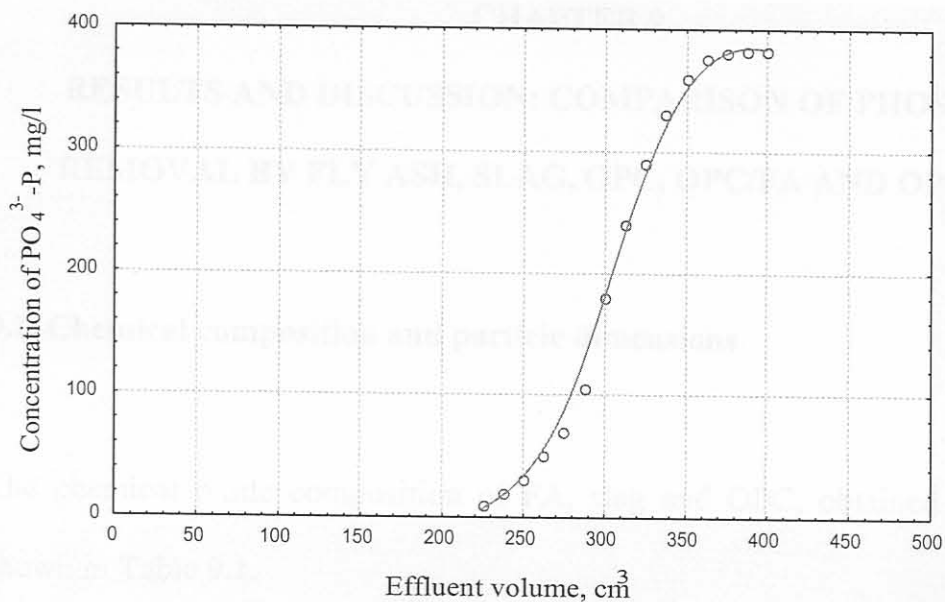


Figure 8.5. Breakthrough curve for PO₄³⁻ removal by OPC/FA.

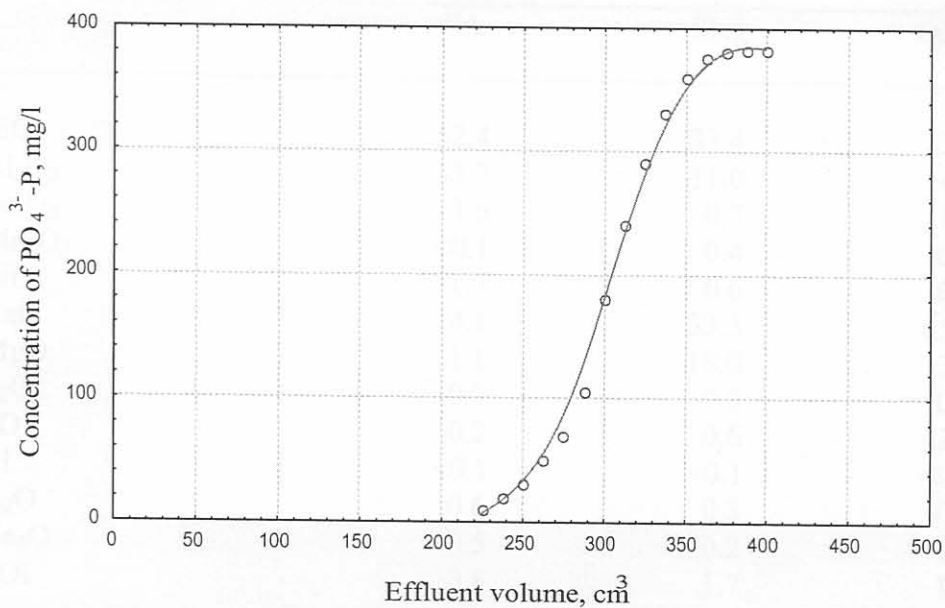


Figure 8.6. Breakthrough curve for PO₄³⁻ removal by OPC/Slag.